Electromagnetic Radiation Source Identification Based on Spatial Characteristics by Using Support Vector Machines

Dan Shi and Yougang Gao

Department of Electronic Engineering
Beijing University of Posts and Telecommunications, Beijing, 100000, China
shidan@buptemc.com

Abstract ─ In the radio monitoring, electromagnetic interference diagnostics and radar detection, the electromagnetic radiation source identification (ERSI) is a key technology. A new method for ERSI was proposed. The support vector machines (SVMs) have been applied to facilitate the ERSI on the basis of the spatial characteristics of the electromagnetic radiation sources. The radiation sources were located by the triangulation method, and then their spatial characteristics were collected by a band receiver array, and converted from 3D data to 1D vector with subscripts as the inputs for the SVMs. We trained the model with these 1D vectors to enable it to identify the radiation source types with both high speed and accuracy. The identification time needs only a few seconds, which is much faster than the artificial neural networks (ANNs). The influence of parameters (e.g., noise from the ambient environment, the data collection method, the scaling method for the input data, and the penalty parameter) were discussed. The proposed method has good performance even in the noisy environments. The results were verified by a designed measurement. The proposed approach is very useful for the ERSI of unknown radiation sources in practice.

Index Terms ─ Band receiver array, electromagnetic radiation source identification, spatial characteristics, support vector machines.

I. INTRODUCTION

Electromagnetic radiation source identification has been a topic of intense researches due to its applications in the radio monitoring and electromagnetic interference diagnostics as well as radar sensor [1-10]. Nowadays, the EMC diagnosis is mainly confronting with a challenge, that is, the identification and localization of different interference sources. The traditional EMC diagnosis widely relies on the experience of engineers and the exact knowledge of the electronic system, and there is no unitized methodology can be referred to. [1] proposed an electromagnetic radiation source identification method based on the independent component analysis (ICA) theory. By using a kurtosis-based ICA algorithm, the radiated emission feature of different sources is extracted from some spectrum data measured at different positions. This method requires that the sources are independent signals, whose features are different frequencies. If the frequencies overlap, the method may be unavailable. Moreover, the accuracy is affected by the noise in the environment significantly. [2-8] investigated the possibility of detecting and identifying the electronic devices based on their electromagnetic emissions. Short-term FFT combined with a cross correlation technique was applied to identify different devices [2]. The signal was separated from the noise on the basis of different frequency, and then the envelope of the signal was recovered. The devices were identified by their envelopes with a cross correlation or a neural network. Thus, the different frequencies and envelopes are necessary for this method. [3] presented a method for detecting and identifying the vehicles based on their RF emissions. The parameters like the average magnitude or the standard deviation of the magnitude within a frequency band were extracted from the measured emission data. These parameters were used as the inputs to the artificial neural networks (ANNs) that were trained to identify the vehicle that produced the emissions. When a spark event was not captured, however, the neural network was unable to successfully identify the responsible vehicle. Thus, a high signal to noise ratio is needed. In the radar detection, many published literatures are focus on the emitter identification (EID). The conventional identification approaches, which separate the received pulses into individual emitter groups, are usually based on the basic pulse parameters, such as the direction of arrival (DOA), radio frequency, time-of-arrival, pulse width and pulse repetition interval; these approaches are not applicable when the EM source frequencies overlap and are sensitive to noise [9-18]. In the radio monitoring, the distinction between the radiation sources mainly depends on the frequency separation by using a spectrum analyzer [19-20].

Our group has been working on the radiation source identification when the frequencies of sources overlap in

Submitted On: September 2, 2016
Accepted On: December 24, 2016

the noisy environment [21-22]. Firstly, we proposed to identify the radiation sources based on their spatial characteristics by using the artificial neural networks [21]. The method is very accurate without any additive noise. However, the accuracy is affected by the noise significantly. Thus, an improved method was brought forward [22]. The radiation source type was recognized by the support vector machines (SVMs), which can withstand some strong noise. Nevertheless, the above two methods have same limitation for they use the same receiver array, which is located in a 3D cube. This requires that the test data must be collected in the same way as the training data collected. It means all data are collected in the enlarged or shrunken cubes in the main lobe of the radiation sources, and only small bias is allowed.

In this paper, to make the method more applicable, the receiver array is improved by using a band shape instead of a 3D cube. The band receiver array is more consistent with the pattern recognition theory. It relaxes the requirement that the test data should be exactly collected in the same way as the training data collected, where all the data are collected in a narrow cone around the main lobe of the radiation sources. In our model, the ERSI problem is considered as a nonlinear mapping problem, the mapping from the space of the feature vectors of the radiation source to the space of the source type. The effectiveness of the method is demonstrated as a multi-ERSI problem with and without the additive noise. With this method, taking the spatial characteristics as the feature vectors is enough to obtain the high accuracy for the identification, which is much simpler than the multi-features for the identification in [9].

II. SVMs FOR CLASSFICATION

The data used for the SVM classification is often a pair comprising an input object (typically a vector, called attribute or feature) and a desired output value (called label). A supervised learning algorithm analyzes the training data and produces inferred functions, which are called "classifiers". The inferred function should predict the correct output value for any valid input object. This approach requires the learning algorithm to generalize unseen situations in a "reasonable" way.

In classification, however, it often happens that the data sets to discriminate are not linearly separable in a finite dimensional space. For this reason, it is proposed that the original finite-dimensional space is mapped into a much higher-dimensional space, presumably making the separation easier in that space. In our model, the data sets composed by the electric field strengths at 27 points are difficult separated in the finite dimensional space, so they should be mapped into a higher-dimensional space by using a kernel function $K(\boldsymbol{x}_i, \boldsymbol{x}_j)$ [23-24]. The radial basis function (RBF), a kind of the kernel functions, is suitable for the case that the class labels and attributes is nonlinear. In our model, the attributes are the electric field strengths at 27 points, and the labels are the types of the radiation sources, so the RBF is chosen for this nonlinear issue;

$$K(\boldsymbol{x}_i, \boldsymbol{x}_j) = \exp(-\gamma \| \boldsymbol{x}_i - \boldsymbol{x}_j \|^2), \ \gamma > 0 . \quad (1)$$

After the data are mapped to a higher-dimensional space with the RBF, the soft margin method will choose a hyper-plane that splits the examples as cleanly as possible, while still maximizing the distance to the nearest cleanly split examples [25]. The method introduces the non-negative slack variables ξ_i to mark a degree of the classification error of sample xi. Given a training set of attribute-label pairs $(\boldsymbol{x}_i, \boldsymbol{y}_i)$, $i = 1, \cdots, m$, where $\boldsymbol{x}_i \in \mathrm{R}n$ and $\boldsymbol{y}_i \in \{-1,1\}^m$, the SVMs require the solution of the following optimization problem:

$$\min_{\boldsymbol{w},b,\xi} \left\{ \frac{1}{2} \boldsymbol{w}^T \boldsymbol{w} + C \sum_{i=1}^{m} \xi_i \right\}$$

$$\text{subject to } \begin{matrix} \boldsymbol{y}_i (\boldsymbol{w}^T \phi(\boldsymbol{x}_i) + b) \geqslant 1 - \xi_i \\ \xi_i \geqslant 0 \end{matrix} . \quad (2)$$

Here, the training vectors $\boldsymbol{x}_i$ are nonlinearly mapped into a higher dimensional space by the function ϕ. The RBF has the relationship with function ϕ, that is, $K(\boldsymbol{x}_i, \boldsymbol{x}_j) = \phi(\boldsymbol{x}_i)^T \phi(\boldsymbol{x}_j)$. $\boldsymbol{w}$ is the normal vector to the hyper-planes. We should minimize $\|\boldsymbol{w}\|$ to find the maximum distance between these hyper-planes. C>0 is the penalty parameter of the error term, and the compromise between the maximal margin and the classification error can be achieved by adjusting C. Eq. (2) tries to increase the margin and decrease the error introduced by ξ_i.

The steps using the SVMs for the classification in this paper are listed below:

1) Collect data sets comprising attributes (electric field strengths at 27 points) and labels (types of the radiation sources), and randomly divide them into the training sets and test sets.
2) Scale the attributes.
   The scaling of attributes is to avoid the attributes in greater numeric ranges to dominate those in smaller numeric ranges, and can accelerate the convergence of the SVMs. Since the kernel values usually depend on the inner products of the feature vectors, large attribute values may also lead to numerical problems. As a result, each attribute is scaled to the range [0, 1] in our model. An arc tangent, logarithm scaling and linear scaling are applied, and the results are compared in Section IV.
3) Choose the RBF kernel function.
   The RBF usually works well in the situation that the

number of feature is small, but the size of the training set is intermediate. For the model introduced in the paper, which contains 27 feature points and 9,000 rows in the training set, the RBF kernel can help provide enough variance to fit the training data within the constraints.

4) Perform cross-validation to find the best parameters C and γ. The influence on identification accuracy from different C and γ is investigated in Section IV. The optimized C and γ are found by the genetic algorithm (GA), which are 2 and 1 respectively in our model.
5) Utilize the best parameters C and γ to train the data sets and then find an appropriate inferred function.
6) Test and predict the accuracy with the test data sets, and then check the validity of the method.

III. MODEL AND CALCULATION

For the intentional electromagnetic radiation, it is often generated from the radiator, namely antenna. For instance, the radiation from a mobile phone usually comes from the phone antenna, such as the planar inverse-F antenna (PIFA), the radiation from a base station is often generated by a planar antenna, and the radars transmit the electromagnetic wave through the phased array antennas, etc. On the other hand, for the unintentional radiation, it is often caused by the equivalent antennas. For example, a bare wire in an electronic device often causes the electromagnetic interference (EMI), which is usually modeled with a dipole antenna. The radiation caused by a printed circuit board trace is often modeled with a loop antenna. In a word, the devices causing the radiation interference can be modeled with their primary radiated antennas. Obviously, the spatial characteristics of different antennas are different, which are unique features used for identification of the antennas, thereby achieving the ERSI.

In [21] and [22], the spatial characteristics of the radiation sources are collected by a 3D cube. The dimensions of this cube are 50 mm x 50 mm x 50 mm. The 27 receivers distributed in a cube are located at the center of edges, faces and volume. Two neighboring receivers are set 25 mm away from each other. The cube moves with a 20 mm steps in the x, y and z directions in a cone around the main lobe to collect the data sets. In those models, the way collecting the data sets for the recognition should be similar with the way collecting data sets for the training. That is, the 27 receivers collect the data sets in the enlarged or shrunken cubes in a narrow cone around the main lobe of the radiation sources. In other words, the high identification accuracy is achieved under these conditions:

(1) The test data sets are collected at the same plane as the training data sets, shown in Fig. 1.
(2) For an alternative method, if the test data sets are collected at different plane from the training data sets, the distance between the neighboring receivers should vary with the distance from the radiation source to the receiver cube, and the formula is presented in [21];

$$L = H/50\sqrt{6}\,, \tag{3}$$

where L is the distance between the neighboring receivers, H is the distance from the radiation source to the receiver cube.

We have tested the ability of the method proposed in [21] to withstand the deviation between the test data sets and the training data sets. It is found that the identification accuracy decreases significantly with the deviation, as shown in Table 1.

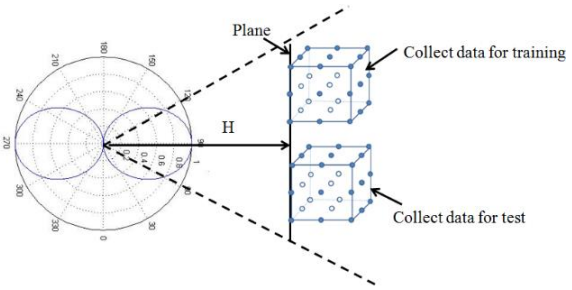

Fig. 1. Data collection for a dipole antenna.

Table 1: Identification accuracy vs. deviation

Training Data Location / Test Data Location	5 m	10 m
1.5 m	13.59%	19.03%
3 m	50.46%	29.37%
5 m	89.86%	46.2%
6 m	78.6%	55.12%
10 m	63.7%	91.49%
15 m	54.94%	71.25%
20 m	51.93%	60.08%

Table 1 shows that the location deviation between the training data sets and the test data sets gives rise to an accuracy degeneration.

To solve the problem, hence, this paper brings up a new receiver array. In practice, before the data are collected by the receiver array, the position of the radiation source should be located. The triangulation method is often used. As Fig. 2 shows, a directional antenna with a narrow range is located at TP1. The DOA (direction of arrival) of the radiation source is determined [26], which is in the line of r1. Similarly, another directional antenna is located at TP2, which determines that the radiation source is in the line of r2. Therefore, the intersection point between r1 and r2 is the location of the radiation source [27].

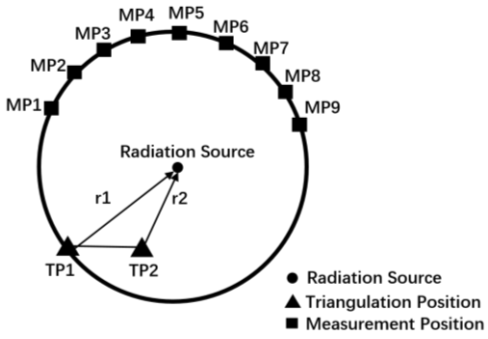

Fig. 2. Triangulation for determining the position of a radiation source.

After the location of the radiation source is determined, the receiver array is moved around the equator of the radiation source to collect the electric field distribution of the source, and then the data are sent to the SVMs for the training and recognition. The steps of the ERSI are shown in Fig. 3.

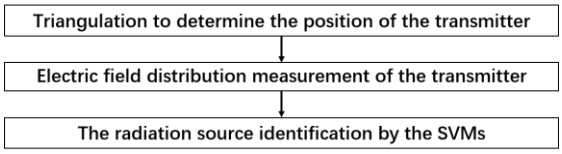

Fig. 3. Steps of ERSI.

The receiver array is composed by 27 elements, which are utilized to collect the spatial characteristics of the radiation source simultaneously. The receivers are located at a band, which is 30° in latitude and 120° in longitude. All the receivers are arranged at 3 rows and 9 columns. The receivers at 9 columns are shown as MP1 to MP9 in Fig. 2. The neighboring receivers are 15° intervals in latitude and 15° intervals in longitude. Then the receiver band moves along the equator of the radiation sources with a 0.1° step. When the band moves 360° along the equator, 3600 data sets are collected, and every data set includes 27 values, which can be expressed as a 1D vector with 27 elements:

$$\boldsymbol{E}_{\mathrm{p}}^{\mathrm{k}} = [\boldsymbol{E}_{11}^{\mathrm{kp}}, \boldsymbol{E}_{12}^{\mathrm{kp}}, \boldsymbol{E}_{13}^{\mathrm{kp}}, \boldsymbol{E}_{14}^{\mathrm{kp}}, \boldsymbol{E}_{\mathrm{mn}}^{\mathrm{kp}} \cdots, \boldsymbol{E}_{39}^{\mathrm{kp}}], \qquad (4)$$

where k is the label of the radiation source type, p is the position label of the band receiver array, m is the row label of the receiver in the band, and n is the column label of the receiver in the band.

Three EM radiation sources, namely, the bare wires, mobile phones, and RFID systems, are modelled with their primary radiators, that is, a dipole antenna, a planar inverse-F antenna (PIFA), and a microstrip antenna, respectively. These three antennas are all working at 3 GHz to ensure that the SVMs identify the radiation sources on the basis of the spatial characteristics other than the frequency. The electric field distributions around these sources, called "spatial characteristics", are collected by the simulation with the HFSS software, a commercial software based on the finite element method [28]. The band receiver arrays vs. the antenna patterns are displayed from Fig. 4 to Fig. 6.

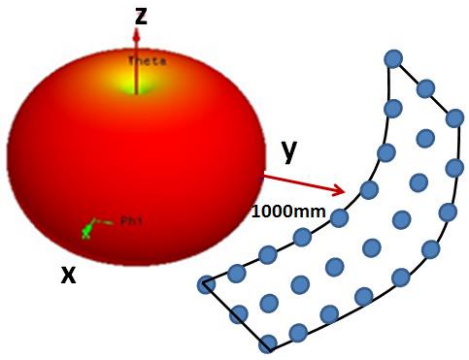

Fig. 4. Receivers vs. pattern of a dipole antenna.

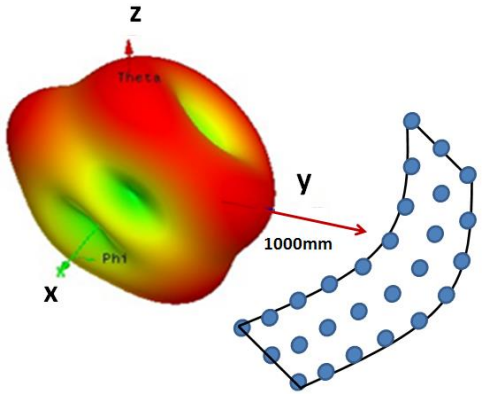

Fig. 5. Receivers vs. pattern of a PIFA antenna.

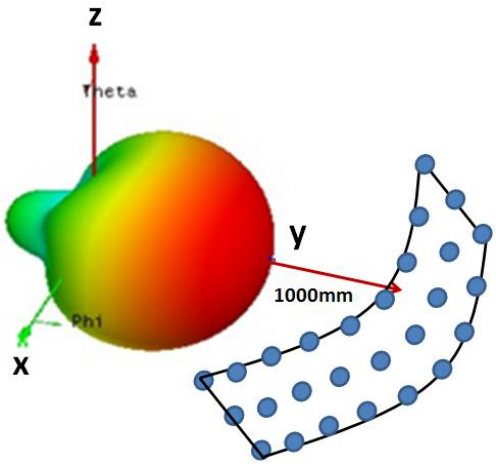

Fig. 6. Receivers vs. pattern of a microstrip antenna.

Obviously, the spatial characteristics of these three antennas are different as shown in Figs. 4-6. They are

collected by a band receiver array, which is a circular and part of a big ring around the radiation source, and are used as the unique features for the SVMs to identify. The spatial information is converted from 3D array to 1D vector with subscripts as inputs to simplify the model. Since there are 3600 data sets, that is, 3600 1D vectors for each antenna, 10800 data sets for these three antennas are obtained. These data sets are expressed as a combined vector set $\boldsymbol{E}_{total} = [\boldsymbol{E}_1^1, \boldsymbol{E}_2^1, \cdots, \boldsymbol{E}_{3600}^3]'$, where the superscript in the vector set represents the type of the radiation source, and the subscript in the vector set represents the position of the band receiver array. The vector set $\boldsymbol{E}_{total}$ is scaled to the range [0, 1] with a linear scaling and marked with the source type. For instance, the data sets belonging to the dipole antenna are marked with "1" at the end of the data sets, the data sets belonging to the PIFA antenna are marked with "2", and the third one is marked with "3". The vector set $\boldsymbol{E}_{total}$ includes 10800 vectors, which are randomly divided into two categories for the training and the test. In the training process, the RBF kernel function is utilized to extract the relationship between the spatial characteristics and the source types, and constructs a hyper-plane classifying the sources based on the vectors. Since the distinction among the spatial characteristics of the radiation sources is apparent, the hyper-plane is easy to construct. The RBF kernel function has two important parameters, called "kernel parameter γ and penalty parameter C". The GA is applied to find the best parameters C and γ by an iteration searching, which are 2 and 1 in this model respectively. After trained with 9000 data sets within a few minutes, the SVMs can identify these EM source types by their spatial characteristics rapidly and accurately. The 1800 data sets left are applied for the test. When the vectors are input into the SVMs, the SVMs can identify the source types these vectors belong to, and the identification accuracy is up to 100%. The $F1$ measure is used for checking the validity of our model. $F1$ combines the recall (r) and the precision (p) with an equal weight in the following form:

$$F1 = \frac{2rp}{r+p}, \tag{5}$$

where p is the number of the correct results divided by the number of all returned results, and r is the number of the correct results divided by the number of results that should have been returned. The $F1$ in this model is 1, which reflects the validity of our method.

IV. DISCUSSION

A. The influence from the noise

In this section, the influence from ambient noise is investigated. The Gaussian noise is added in our model. The parameter of signal-to-noise ratio (SNR) is applied, which is expressed as follows:

$$\text{SNR (dB)} = 10 \times \log_{10} \frac{P_{\text{avg}}}{P_{\text{noise}}}, \tag{6}$$

where P_{avg} is the average power of the input data, and P_{noise} is the power of the Gaussian noise.

The identification accuracy versus SNR is listed in the Table 2. It also gives the comparison between the SVMs and the ANNs. The ANNs are classic back-propagation (BP) neural networks which include one input layer, one hidden layers, and one output layer. There are 30 neurons in the hidden layer. The levenberg-marquardt algorithm is applied in the training. When the mean square error (MSE) falls below 0.01 or the epochs exceed 30000, the training stops. The data for the training and the test are same with those for the SVMs, and a linear scaling is used. From Table 2 it is found that if no noise is added, the identification accuracy with the SVMs and the ANNs is both very high. However, the SVMs are not closely related to the noise. When the SNR decreases from 20 dB to 15 dB, the accuracy varies from 99.94% to 97.12%. Even in a strong noise environment, where the SNR is only 10 dB, the accuracy with the SVMs is still 76.57%. Thus, the method using the SVMs to identify the radiation sources can be applied in the noisy environments. Whereas the accuracy with the ANNs significantly decreases as the noise increases. When the SNR is 15 dB, the accuracy rate with the ANNs degrades to 64.1%, and it cannot work when the SNR is 10 dB.

Table 2: Identification accuracy vs. SNR

SNR/dB	No Noise	25	20	15	10
Accuracy of SVMs/%	100	100	99.94	97.12	76.57
Accuracy of ANN/%	99.98	98.43	82.3	64.1	38.87

B. The influence from the data collection

The spatial characteristics are represented by the data sets. Thus, the method of the data collection is important to the identification accuracy. In [22], we proposed to collect the data sets by using a 3D cube with 27 receivers. The 3D cube moves along a cone, whose angle is 60°. So the data sets mainly represent the spatial characteristics of the main lobe of the antennas. As an improved method, the data sets are collected with a band receiver array, and the band moves around the equator of antennas. According to the pattern recognition theory, it is preferable to identify the radiation sources with the global information other than the local information, which has been proven by the result comparison between this method and that proposed in [22].

Some other test results also support this point. Firstly, we use a band receiver array with 9 receivers to collect the data sets. The neighboring receivers are 1° intervals in longitude. The identification accuracy is not good, and the best accuracy is only 71.2%. So we

suppose that the receiver number is not enough to collect the spatial characteristics. Then the receiver number is increased to 30, and the neighboring receivers are also 1° intervals in longitude. Unfortunately, the identification accuracy is still not satisfactory. Thus, we increase the intervals between the neighboring receivers to 15° in longitudes and 27 receivers are applied, and good results are obtained finally. The reason lies in the fact that the pattern recognition has better performance when the object is recognized as a whole. The results using a receiver array with different intervals are compared in Fig. 7.

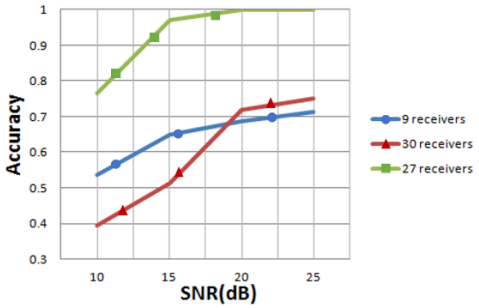

Fig. 7. Accuracy of three data collection methods.

From Fig.7 it can be found that the method using 27 receivers with 15° intervals is the most accurate one among these three methods.

C. The influence from the scaling method

Different scaling methods give different identification accuracy. In this section, three typical scaling methods, namely the tangent scaling, logarithm scaling and linear scaling, are utilized to investigate the influence from the scaling method on the accuracy.

As mentioned in Section III, a total of 10800 input vectors are expressed as a combined vector set $\boldsymbol{E}_{total} = [\boldsymbol{E}_1^1, \boldsymbol{E}_2^1, \cdots, \boldsymbol{E}_{3600}^3]'$. The elements in $\boldsymbol{E}_{total}$ are scaled by three different methods.

The following formula is applied for the arc tangent scaling:

$$\boldsymbol{E}_s = a\tan(\boldsymbol{E}_{total}) \times 2/\pi , \tag{7}$$

where $\boldsymbol{E}_s$ is the input vector sets after the scaling.

Eq. (8) is used for the logarithm scaling:

$$\boldsymbol{E}_s = \log_{10}(\boldsymbol{E}_{total}) . \tag{8}$$

Eq. (9) is applied for the linear scaling:

$$\boldsymbol{y}_i = \frac{\boldsymbol{x}_i - x_{\min}}{x_{\max} - x_{\min}} , \tag{9}$$

where $\boldsymbol{x}_i$ is the element of $\boldsymbol{E}_{total}$; $\boldsymbol{y}_i$ is the element of $\boldsymbol{E}_s$ after the scaling; $x_{\max}$ and $x_{\min}$ are the maximum and minimum elements of $\boldsymbol{E}_{total}$, respectively.

The accuracy versus different scaling methods is shown in Table 3.

Table 3: Accuracy vs. scaling method

SNR/dB	25	20	15	10
Accuracy with arc tangent scaling/%	95.09	93.66	84.16	67.21
Accuracy with logarithm scaling/%	100	99.47	92.4	68.67
Accuracy with linear scaling/%	100	99.94	97.12	76.57

Obviously, the linear scaling method has the best performance among these three scaling methods. The reason lies in the fact that the linear scaling works better when the data value exceeds 3 while the arc tangent scaling is more suitable for the data value in range (0-3), and most of the data used in our model are above 4.

D. The influence from the parameters of the SVMs

For the support vector machines, there are two key parameters, namely the penalty parameter C and γ of the kernel function. The penalty parameter C reflects the impact from the outlier case, and adjusting it can achieve the compromise between the maximal margin and the classification error. According to Eq. (2), the loss of the object function increases with C when $\sum_{i=1}^{m} \xi_i$ is fixed. When C is infinite, the problem would be insoluble once the outlier case exists. Therefore, smaller C is preferable when the same identification rate is achieved since it can improve the generalization ability of the SVMs. However, if C is too small, the penalty to the outlier case is small and the error is large, leading to an identification accuracy degradation. For γ of the kernel function, it represents the correlation between those support vectors. If γ is too small, there is no significant correlation between the support vectors, and the learning process is complex. On the other hand, if γ is too large, the mutual influence between the support vectors is obvious and the precision of the model will be affected. Table 4 presents the identification accuracy versus C and γ . The optimized C and γ are found by the GA, which are 2 and 1 respectively. Obviously, the most accurate result is obtained with these optimized parameters. The accuracy decreases as the values of C and γ deviate from the optimized values. If the C and γ are too small or too large, the accuracy is poor.

Table 4: Accuracy vs. parameters

Parameters	C=0.1, γ=0.1	C=0.2, γ=0.2	C=2, γ=1	C=20, γ=20	C=100, γ=100
Accuracy/%	79.61	94.66	100	89.58	35.62

V. VERIFICATION BY MEASUREMENTS

Some measurements are made to validate the proposed method. The spatial characteristics of the three cell phones with above antennas are collected by a receiving antenna and a spectrum analyzer in an anechoic chamber. The electric field of the points distributed within the sphere that surrounds the source can be obtained by setting the rotation angle of the receiving antenna. A 1° interval is applied for the antenna rotation in the equatorial plane, and 15° intervals are used in the meridian plane. Consequently, the data within the band from −15° to 15° longitude and 1° to 360° latitude around the cell phones are extracted. Then, the electric fields at 27 points are divided into groups using the same method described in Section III. A total of 90 data sets are selected randomly from the three cell phones (i.e., 30 for each cell phone), combined, and scaled. Finally, the scaled data are sent to the proposed model to check the validity of the presented method. The model can correctly identify the data set belonging to which type of the sources. The identification accuracy is 96%, which proves the validity of the proposed method.

VI. CONCLUSION

A new method for the ERSI by using the SVMs is proposed in this paper. The data collection method has been improved. After the position of the radiation source is determined by the triangulation method, a band receiver array is applied for the data collection. The band receiver array moves along the equator of the radiation sources and focuses on collecting the data with global information, which more coincides with the pattern recognition. The results demonstrate that the method proposed in this paper has a better identification accuracy compared with the ANNs and the 3D cube receiver array. It can be applied in a strong noise environment, and the deviation between the training data sets and the test data sets is allowed.

In practice, the method proposed in this paper is also useful for the radiation predication of the sources. The same SVMs model can be applied. After trained by the electric field strengths at several points, the SVMs can predict all the radiations from the sources accurately, which can save a lot of computation time and cost, and this will be investigated in the next step.

ACKNOWLEDGMENT

This work has been supported by National Natural Science Foundation of China, No. 61201024.

REFERENCES

[1] Z. F. Song and D. L. Su, "A novel electromagnetic radiated emission source identification methodology," *Proceeding of 2010 Asia-Pacific International Symposium on* Elec*tromagnetic Compatibility*, pp. 645-648, 2010.

[2] H. Weng, X. Dong, X. Hu, D. G. Beetner, T. Hubing, and D. Wunsch, "Neural network detection and identification of electronic devices based on their unintended emissions," *International Symposium on EMC*, vol. 1, pp. 245-249, 2005.

[3] X. Dong, H. Weng, and D. G. Beetner, "Detection and identification of vehicles based on their unintended electromagnetic emissions," *IEEE Transaction on Electromagnetic Compatibility*, vol. 48, no. 4, pp. 752-759, 2006.

[4] T. Hubing, D. Beetner, X. Dong, H. Weng, M. Noll, B. Moss, and D. Wunsch, "Electromagnetic detection and identification of automobiles," *Proceeding of EuroEM*, Magdeburg Germany, July 2004.

[5] H. Weng, X. Dong, X. Hu, D. Beetner, T. Hubing, and D. Wunsch, "Neural network detection and identification of electronic devices based on their unintended emissions," *in Proc. IEEE Int. Symp. Electromagn. Compat.*, 2005, vol. 1, pp. 245-249, 2005.

[6] C. J. Kaufman, J. Dudczyk, J. Matuszewski, and M. Wnuk, "Applying the radiated emission to the specific emitter identification," *in Proc. 15th Int. Conf. Microwave, Radio Wireless Commun.*, Warsaw, Poland, vol. 2, pp. 431-434, May 17-19, 2004.

[7] M. D'Amore, A. Morriello, and M. S. Sarto, "A neural network approach for identification of EM field sources: Analysis of PCB configurations," *in Proc. IEEE Int. Symp. Electromagn. Compat.*, Denver, CO, vol. 2, pp. 664-669, Aug. 24-28, 1998.

[8] K. Aunchaleevarapan, K. Paithoonwatanakij, Y. Prempreaneerach, W. Khanngern, and S. Nitta, "Classification of PCB configurations from radiated EMI by using neural network," *in Proc. CEEM*, Shanghai, China, pp. 105-110, May 3-7, 2000.

[9] C.-S. Shieh and C.-T. Lin, "A vector neural network for emitter identification," *IEEE Trans. Antennas Propag.*, vol. 50, no. 8, pp. 1120-1127, Aug. 2002.

[10] H. Liu, Z. Liu, and W. Jiang, "Approach based on combination of vector neural networks for emitter identification ," *IET Signal Processing*, vol. 4, no.2, pp. 137-148, 2010.

[11] H. Liu, Z. Liu, and W. Jiang, "Incremental learning approach based on vector neural network for emitter identification," *IET Signal Pro*cessing, vol. 4, no.1, pp. 45-54, 2010.

[12] L. Li, H. B. Ji, and L. Jiang, "Quadratic time-frequency analysis and sequential recognition for specific emitter identification," *IET Signal Processing*, vol. 5, no. 6, pp. 568-574, 2011.

[13] M. Wnuk, A. Kawalec, and J. Dudczyk, "The

method of regression analysis approach to the specific emitter identification," *Proceeding of 16th International Conference on Microwaves, Radar and Wireless Communications*, Krakow, Poland, pp. 491-494, May 22-24, 2006.

[14] X. Chen and W. D. Hu, "Approach based on interval type-2 fuzzy logic system for emitter identification," *Electronics Letters*, vol. 48, no. 18, 2012.

[15] M. Liu and J. F. Doherty, "Nonlinearity estimation for specific emitter identification in multipath channels," *IEEE Transactions on Information Forensics and Security*, vol. 6, no. 3, pp. 1076-1085, 2011.

[16] H. Ye, Z Liu, and W. Jiang, "Comparison of unintentional frequency and phase modulation features for specific emitter identification," *Electronics Letters*, vol. 48, iss. 14, pp. 875-877, 2012.

[17] L. Anjaneyulu, N. S. Murthy, and N. Sarma, "Radar emitter classification using self-organising neural network models," *Proceedings of International Conference on Recent Advances in Microwave Theory and Applications*, Jaipur, Rajasthan, India, pp. 431-433, Nov. 21-24, 2008.

[18] Y. Zhang, H. P. Zhao, and Q. Wan, "Single snapshot 2D-DOA estimation in impulsive noise environment using linear arrays," *ACES Journal*, vol. 27, no. 12, pp. 991-998, 2012.

[19] F. Mavromatis, A. Boursianis, T. Samaras, C. Koukourlis1, and J. N. Sahalos, "A broadband monitoring system for electromagnetic-radiation assessment," *IEEE Antennas and Propagation Magazine*, vol. 51, iss. 1, pp. 71-79, 2009.

[20] C. Camilo Rodríguez, C. Andrés Forero, and H. Ortega Boada, "Electromagnetic field measurement method to generate radiation map," *IEEE Colombian Communications Conference*, pp. 1-7, 2012.

[21] D. Shi and Y. G. Gao, "A new method for identifying electromagnetic radiation sources using backpropagation neural network," *IEEE Transactions on Electromagnetic Compatibility*, vol. 55, iss. 5, pp. 842-848, 2013.

[22] D. Shi and Y. G. Gao, "A method of identifying electromagnetic radiation sources by using support vector machines," *China Communications*, vol. 10, iss. 7, pp. 36-43, 2013.

[23] C. Nello and S.-T. John, *An Introduction To Support Vector Machines And Other Kernel-based Learning Methods*. Cambridge University Press, 2000.

[24] B. Schölkopf, C. J. C. Burges, and A. J. Smola, *Advances In Kernel Methods: Support Vector Learning*. MIT Press, Cambridge, MA, 1999.

[25] C. Cortes and V. Vapnik, "Support-vector networks," *Machine Learning*, vol. 20, no. 3, pp. 273-297, 1995.

[26] Q. Yuan, Q. Chen, and K. Sawaya, "Accurate DOA estimation using array antenna with arbitrary geometry," *IEEE Transactions on Antennas and Propagation*, vol. 53, no. 4, pp. 1352-1357, 2005.

[27] A Practical Approach to Identifying and Tracking Unauthorized 802.11 Cards and Access Points. http://www.interlinknetworks.com/graphics/news/wireless_detection_and_tracking.pdf

[28] ANSYS[EB/OL]. http://www.ansys.com/Products/Simulation+Technology/Electromagnetics/High-Performance+Electronic+Design/ANSYS+HFSS

Dan Shi received Ph.D. degree in Electronic Engineering from Beijing University of Posts & Telecommunications, Beijing, China in 2008.

She has been working in Beijing University of Posts & Telecommunications. Her interests include electromagnetic compatibility, electromagnetic environment and electromagnetic computation.

Shi has published more than 100 papers. She is Chair of IEEE EMC Beijing Chapter, Vice Chair of URSI E-Commission in China, General Secretary of EMC Section of China Institute of Electronics.

Yougang Gao received his B.S degree in Electrical Engineering from National Wuhan University, China in 1950. He was a Visiting Scholar in Moscow Technical University of Communication and Information in Russia from 1957 to 1959. He is now a Professor and Ph.D. Supervisor in Beijing University of Posts and Telecommunications, China. He has been an Academician of International Informatization Academy of UN since 1994. He was once the Chairman of IEEE Beijing EMC Chapter and Chairman of China National E-Commission for URSI. He has published several books: Introduction of EMC, Inductive Coupling and Resistive Coupling, as well as Shielding and Grounding (all these books were published by People's Posts and Telecommunications Press). He became an EMP Fellow of US Summa Foundation since 2010.